Effects of uniform magnetic induction on heat transfer performance of aqueous hybrid ferrofluid in a rectangular cavity

S.O. Giwa, M. Sharifpur* and J.P. Meyer

Department of Mechanical and Aeronautical Engineering, University of Pretoria, Pretoria 0002, South Africa

∗Corresponding author. E-mail address: mohsen.sharifpur@up.ac.za (M. Sharifpur).

Highlights

- Aqueous hybrid ferrofluid (AHF) has been investigated for the heat transfer capability in a rectangular cavity under magnetic induction.
- Effective viscosity and thermal conductivity of stable AHF was measured for different volume concentrations.
- Correlations were proposed for the effective viscosity and thermal conductivity of AHF.
- Heat transfer was augmented at lower volume concentrations of AHF in the absence of magnetic induction.
- •In the presence of magnetic induction, heat transfer of AHF was further augmented.

Abstract

Utilization of hybrid nanoparticles to formulate nanofluids is one of the ways to improve nanofluids' thermal and fluid properties. This work attempted to study the free convection heat transfer performance of aqueous Fe_2O_3-Al_2O_3 (75:25) nanofluids in a rectangular cavity under magnetic induction. The thermal properties of the aqueous hybrid ferrofluids (AHFs) were measured for volume concentrations of 0.05–0.3 vol% and temperatures of 20–40 °C. Also, the stability and morphology of AHFs were examined. On charging the AHF and base fluid samples into the cavity, the two opposite vertical walls were subjected to temperature gradients ranging from 20 to 35 °C to create buoyancy. Parameters such as Nu_{av}, h_{av}, Ra and Q_{av} were determined for each AHF sample and the base fluid. The AHF with the highest heat transfer performance was exposed to magnetic induction to investigate its convective heat transfer. With Ra range of 1.65×10^8–3.80×10^8, the Nu_{av} was observed to intensify with increasing Ra. Without the magnetic induction, the improvements in h_{av}, Nu_{av}, and $\dot{Q}_{av}$ were observed for 0.05–0.2 vol% AHFs in comparison with the base fluid. Optimum heat transfer enhancement of 10.79% was achieved for 0.10 vol% HF at ΔT = 35 °C. By inducing magnetic field (118.4 G) vertically on the side wall of the cavity, a maximum enhancement of Nu_{av} (4.91%) was achieved compared to the case without magnetic induction. Additionally, increasing the magnetic field strength (48.9–219.5 G) was noticed to further enhance heat transfer of 0.10 vol% AHF. Correlations were proposed for predicting viscosity, thermal conductivity and Nu_{av} of AHF in a rectangular cavity. The use of hybrid nanofluid was revealed to have better heat transfer performance than mono-particle nanofluids. Conclusively, the heat transfer performance was observed to depend on φ, ΔT, AHF deployment, magnetic induction, strength and direction.

Keywords: Aqueous hybrid ferrofluids; Free convection; Heat transfer; Al_2O_3; Fe_2O_3; Cavity; Magnetic induction

Nomenclature

X	percent weight of nanoparticles' type, %	β	thermal expansion coefficient, 1/K
M	mass of nanoparticles' type, g	φ	volume concentration
κ	thermal conductivity, W/mK	φ_w	weight concentration
C_p	specific heat capacity (at constant pressure), J/kgK	μ	viscosity, mPas
T	temperature, °C	Δ	change
A	area of cavity, m^2	*Subscript*	
$\dot{m}$	mass flow rate, kg/s	c	cold side
$\dot{Q}$	heat transfer, W	av	average
g	gravitational acceleration, m^2/s	HF	hybrid ferrofluid
L	characteristic length of cavity, m	DIW	deionized water
Ra	Rayleigh number	Fe_2O_3	hematite nanoparticles
Nu	Nusselt number	Al_2O_3	alumina nanoparticles
h	average coefficient of heat transfer, W/m^2K	i	in
Pr	Prandtl number, $C_p\mu/K$	o	out
H	height, m	h	hot side

Greek symbols

ρ	density of nanoparticles, kg/m^3

1. Introduction

Natural convection hasfound huge and numerous applications in electronics cooling, power generation, nuclear energy, solar energy collectors, agriculture, geophysics, industrial, etc., [1], [2]. In the past two decades, nanofluids have been widely researched and established to possess improved thermal properties when compared with traditional fluids of liquids [2], [3] and air [4], [5]. By extension, the thermo- and thermomagnetic convection of different types of nanofluids in various shapes of cavities have been investigated and still on-going [6], [7], [8], [9], [10], [11], [12], [13]. Published articles in the public domain evidently showed that extensive researches had been conducted in this field of study with great emphasis on the numerical approach relative to the experimental method [14].

Studies on the experiment-based free convection of nanofluids in enclosures of various configurations have been investigated. Putra et al. [15] pioneered the study on the free convection of nanofluids in an enclosure. They considered distilled water (DIW)-based Al_2O_3 and CuO nanofluids (φ = 1–4 vol%) filled into a differentially-heated horizontal cylinder with aspect ratios (ARs) of 0.5–1.5. The result showed the deterioration of heat transfer for all the nanofluids as a function of AR, nanoparticles' density and φ. Li et al. [16] engaged ZnO/DIW-EG (75:25, 85:15, and 95:5 vol%) nanofluid with φ_w = 5.25 wt% in a square enclosure and reported the attenuation of heat transfer for the nanofluids with the increase in EG quantity. Hu et al. [17] used TiO_2-DIW (3.85–10.71 wt%) nanofluid in a vertical square and observed heat transfer deterioration of the same in comparison with the DIW. The work of Kouloulias et al. [18] engaged Al_2O_3/water (0.01–0.12 vol%) nanofluid in a square cavity and also found that the use of nanofluid led to the deterioration of heat transfer compared with the water. A recent study by Ilyas et al. [19] employed MWCNT/thermal oil (0–1 wt%) nanofluid in a vertical rectangular cavity (AR = 4) and revealed that h and Nu depreciated as φ increased. These studies emphasized that the deterioration in the heat transfer capabilities of the investigated nanofluids was mainly due to the increase in viscosity (as φ increased) than other factors such as stability, thermal conductivity, and natural convection of base fluid.

Apart from the findings that the use of nanofluids caused deterioration of heat transfer in comparison with the base fluids, some studies have shown that nanofluids can enhance heat

transfer at specific volume concentrations. Ghodsinezhad et al. [9] reported the enhancement of h by 15% for φ = 0.1 vol% when the thermo-convection behaviour of Al_2O_3/DIW (0.05–0.6 vol%) nanofluid in a differentially heated rectangular was studied. Garbadden et al. [20] used MWCNT/DIW (0–1 vol%) nanofluid in a square enclosure and observed optimal heat transfer performance (45%) when φ = 0.1 vol%. Ho et al. [21] studied the free convection heat transfer in a square cavity containing Al_2O_3/distilled water (DW) (0.1–4 vol%) nanofluid and they demonstrated that the highest heat transfer enhancement occurred for φ = 0.1 vol%. The work of Joshi and Pattamatta [8] was also found to be consistent with those stated above. Relative to DW, they noticed that the maximum improvement in heat transfer was noticed for φ = 0.1 vol% when the thermo-convection performance of Al_2O_3, MWCNT, and graphene/DW (0.1–0.5 vol%) nanofluids filled into a square enclosure was investigated. On the contrary, Nnanna et al. [22] reported that the optimum heat transfer enhancement of Al_2O_3/DIW (0.2–8 vol%) nanofluid contained in a rectangular cavity was achieved when φ = 0.2 vol%. Similarly, Sharifpur et al. [23] found that the free convection heat transfer performance of TiO_2/DIW (0.05–0.8 vol%) nanofluid in a rectangular cavity was augmented by 8.2% at φ = 0.05 vol%.

In attempting to enhance free convection performance of nanofluids in cavities, various techniques such as AR, magnetic field, cavity inclination, hybrid nanofluid (nanofluid prepared using two or more nanoparticles), base fluid, porous cavity, and bio-nanofluid have been employed in experimental studies. The free convection heat transfer characteristics of aqueous carboxymethyl cellulose-based Al_2O_3 and TiO_2 nanofluids in a vertical cylinder with AR = 0.5–1.5 and heated from the bottom was investigated by Mahrood et al. [24]. The result showed that the optimum heat transfer occurred at φ = 0.1 vol% and 0.2 vol% for the TiO_2 and Al_2O_3 nanofluids, respectively, with the former being the better of the nanofluids. For both nanofluids, an increase in AR was observed to augment heat transfer. A rectangular cavity filled with Al_2O_3/DIW (0.01 and 0.1 vol%) nanofluid and having AR = 0.3–2.5 was examined by Choudhary et al. [25]. The free convection heat transfer performance was found to depend on the AR, Ra, and φ. The highest enhancement (29.5%) was recorded for 0.01 vol% at AR = 0.5 and $Ra = 7.89 \times 10^8$. Solomon et al. [26] engaged Al_2O_3/DIW (0.1–0.6 vol%) nanofluid in a cavity having AR of 1, 2 and 4 and noticed that h and Nu were functions of AR. Maximum heat transfer enhancements were achieved when φ = 0.1, 0.2 and 0.3 vol% for cavities with AR = 1, 2 and 3, respectively. Additionally, Ali et al. [27] studied the free convection of Al_2O_3/DW (0.21–0.75 vol%) nanofluid in a vertical cylinder (with AR = 0.0635 and 0.127) heated from the top. They reported the deterioration of the heat transfer performance of the nanofluid as a function of AR and φ with the DW. In a similar study that used the same experimental setup but heated the vertical cylinder from the bottom, Ali et al. [28] showed enhancements of h by 40% and 8% for φ = 0.21 vol% and AR = 0.0635, and φ = 0.51 vol% and AR = 0.127, respectively.

The dual effect of cavity inclination and AR on the augmentation of heat transfer of nanofluids in enclosures were also studied. Moradi et al. [29] experimented the influence of inclination angle (30°–90°), AR (0.5–1.5), and heat fluxes (500–1500 W/m^2) on the free convection characteristics of Al_2O_3/DIW and TiO_2/DIW nanofluids (φ = 0.1–1.5 vol%) in a cylindrical cavity heated from the bottom wall. They showed deterioration of heat transfer with the use of TiO_2/DIW nanofluid and it enhancement when Al_2O_3/DIW nanofluid was engaged. The highest enhancement was observed for φ = 0.2 vol% when AR = 1 and inclination angle = 30°. The presence of porous media in a rectangular cavity saturated with Al_2O_3/EG (60%)-DIW (40%) nanofluid (φ = 0.05–0.4 vol%) was investigated for the free convection heat transfer capability [30]. Results revealed that the heat transfer augmentation depended on the φ and porous media. Concerning the base fluid, the use of the porous media and nanofluid in the cavity yielded heat transfer augmentation of 10% when φ = 0.1 vol% and ΔT = 50 °C.

Giwa et al. [31] pioneered the experimental study of free convection behaviour of hybrid nanofluids of Al_2O_3-MWCNT (95:5 and 90:10)/DIW) with φ = 0.1 vol% in a square cavity. Results revealed the enhancement of heat transfer using hybrid nanofluids when compared with DIW and mono-particle nanofluid of Al_2O_3/DIW [9]. Maximum improvement of h = 9.8% and Nu = 19.4% was achieved using Al_2O_3-MWCNT (90:10 ratio)/DIW nanofluid. An extension of this work in which different percent weights of water-based Al_2O_3-MWCNT nanofluids has been recently published [32]. Additionally, Solomon et al. [33] investigated the free convection of green nanofluid (DIW-based mango bark) with φ = 0.01–0.5 vol% in a rectangular cavity for the first time. They reported the deterioration of the free convection heat transfer of the green nanofluid in comparison to DIW.

Yamaguchi et al. [34] experimented the influence of an external magnetic field on the free convection behaviour of Mg-Zn ferrite/kerosene nanofluid in a square cavity. They showed that the presence of a magnetic field resulted in heat transfer enhancement and increasing the magnetic field strength caused further enhancement. In a similar study by the author and engaging the same magnetic nanofluid, the dual presence of external magnetic field and heat-generating objects (inside the cavity) were observed to augment the free convection heat transfer. Increasing the size of the heat-generating objects was noticed to reduce heat transfer slightly [12]. The influence of φ and three types of arrangements of permanent magnets on the free convection performance of DIW-based Fe_2O_3 nanofluid (0.05–0.3 vol%) contained in a rectangular cavity was examined by Joubert et al. [35]. They observed that the heat transfer augmentation of the nanofluid depended on the φ, magnetic field strength and magnets' configuration. The optimum heat transfer performance was attained when φ = 0.1 vol% with the placement of 700 G magnets above and below the hot side of the cavity. In the presence of the magnetic field, the Nu was enhanced by 2.81% (φ = 0.1 vol%) compared to the case without the magnetic field. Roszko and Fornalik-Wajs [13] researched into the influence of ΔT (5–25 °C), magnetic excitation and strength (0–10 T) on the free convection characteristics of DW-based Ag nanofluid (φ = 0.1 vol%) in a cubic cavity exposed to a variable magnetic field. They showed that the Nu was enhanced as a function of ΔT, magnetic field and strength. Recently, Dixit and Pattamatta [36] examined the influence of magnetic excitation on the free convection of non-magnetic nanofluids (SiO_2/, MWCNT/, graphene/, and Cu/DW) for φ = 0.057–2 vol% in a square cavity. They reported heat transfer depreciation for all the nanofluids considered on exposure to the magnetic field despite indicating enhancement capabilities (for φ = 0.1 vol% MWCNT/DW and graphene/DW nanofluids) when not exposed to the magnetic field. The depreciation was observed to depend on the magnetic field direction and strength, type and concentration of nanofluids and Ra. The work of Dixit and Pattamatta [36] contradicted that of Roszko and Fornalik-Wajs [13] concerning the enhancement of free convection heat transfer of non-magnetic nanofluids in a square enclosure under a magnetic field.

In the context of this literature survey, it is obvious that despite limited experimental studies on the free convection thermal transfer of nanofluids in enclosures, no work at present has reported the synergetic effect of employing the duo of the magnetic field and hybrid nanofluid on heat transfer enhancement. This current study aimed at expanding the body of knowledge on the engagement of both magnetic hybrid nanofluid (hybrid ferrofluid) and magnetic excitation to enhance thermo-convection heat transfer in a cavity. Hybrid nanofluid is an extension of mono-particle nanofluid which is presently being researched as a newly engineered fluid.

2. Experimental study description

2.1. Formulation and characterization hybrid ferrofluids

The nanoparticles used in this study were γ-Al_2O_3 (20–30 nm diameter) and Fe_2O_3 (98% purity; 20–30 nm diameter). Both nanoparticles were purchased from Nanostructured and Amorphous Materials Inc., Houston, Texas, USA. The surfactant (sodium dodecyl sulphate (≥98.5% purity)) was sourced from Sigma-Aldrich, Germany. To formulate the aqueous hybrid ferrofluids (AHFs), Al_2O_3 (25 wt%) and Fe_2O_3 (75 wt%) nanoparticles were dispersed into deionized water (DIW) using the two-step technique. In the formulation of stable AHFs, variables such as dispersion fraction, sonication time, and amplitude were optimized by monitoring the electrical conductivity of AHF. This was used to determine the critical micelle concentration (CMC). The optimized dispersion fraction for the formulation of AHF is provided in Fig. 1. The electrical conductivity was observed to increase until it decreased at the dispersion fraction of 1.1. This point was the CMC, and it was the optimum dispersion fraction for the AHF formulation. Other optimal variables used to achieve stable AHFs were sonication time of 2 h and amplitude of 70% with 5 s and 2 s sonic switching on and off, respectively. The digital weighing balance (Radwag AS 220.R2) was used to weigh Al_2O_3 and Fe_2O_3 nanoparticles, and surfactant (1.1% dispersion fraction). The expression in Eq. (1) was used to estimate the weights of the hybrid nanoparticles and the surfactant dispersed into 1.4 l for various volume concentrations (0.05–0.3 vol%). The weighed materials were put in a beaker and immersed in a water bath (LAUDA ECO RE1225) to maintain a constant temperature while homogenizing the mixture with the use of an ultrasonicator (Qsonica Q-700; 700 W and 20 kHz) at the optimized values for sonication. Stability of the formulated AHFs was monitored using a UV–visible spectrophotometer (Jenway; model 7315) to measure the absorbance for 50 h, and the visual inspection was performed weekly for a month [26]. Also, a transmission electron microscope (JEOL JEM-2100F) was used to characterized the morphology of AHFs.

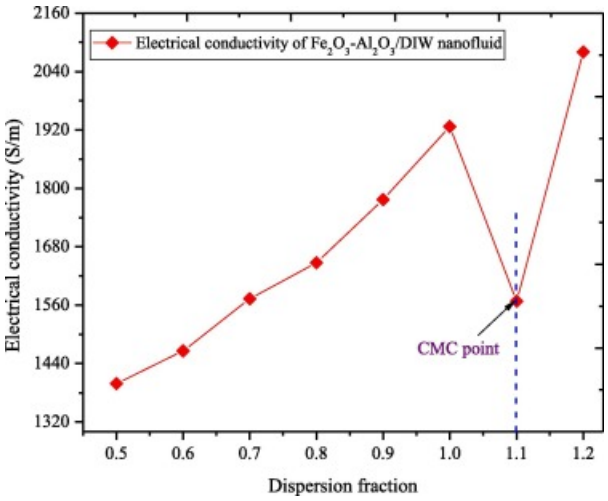

Fig. 1. Optimum dispersion fraction for a stable aqueous hybrid ferrofluid formulation.

$$\varphi = \left(\frac{X_{Fe_2O_3}\left(\frac{M}{\rho}\right)_{Fe_2O_3} + X_{Al_2O_3}\left(\frac{M}{\rho}\right)_{Al_2O_3}}{X_{Fe_2O_3}\left(\frac{M}{\rho}\right)_{Fe_2O_3} + X_{Al_2O_3}\left(\frac{M}{\rho}\right)_{Al_2O_3} + \left(\frac{M}{\rho}\right)_{bf}} \right) \quad (1)$$

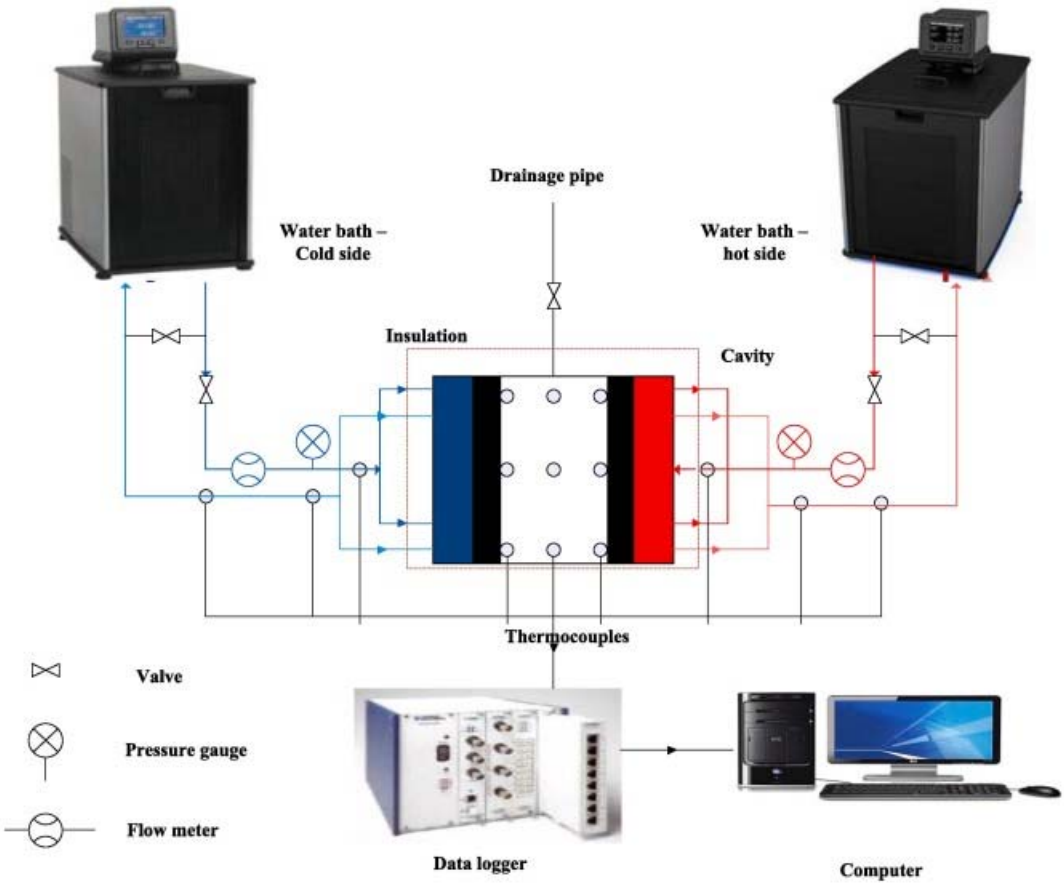

Fig. 2. Experimental setup.

2.2. Description of setup and procedure

The natural convection heat transfer of the AHFs in a rectangular (length 120.8 mm × breadth 99.7 mm × height 113.2 mm) cavity exposed to magnetic excitation was studied. Two opposite vertical walls of the cavity were differentially heated while the remaining walls were thermally insulated. With the temperature differences of 20 °C (20 °C and 40 °C), 25 °C (20 °C and 45 °C), 30 °C (15 °C and 45 °C), and 35 °C (15 °C and 50 °C), natural convection was generated inside the cavity when charged with DIW and AHFs. Isothermal counter-flow shell and tube heat exchangers were engaged in achieving constant heating of the cavity walls by circulating water at constant temperatures between the thermal baths (PR20R-30 Polyscience; −30 and 200 °C; 0.005 °C accuracy) and the heat exchangers. Flow meters (Burkert Type 8081; the accuracy of ±0.01% of full-scale flow rate +2% (measured value)) installed on the inlet pipes of the heat exchangers were used to measure the flow rates of the water being circulated. Both the pipe connections and the cavity were insulated to reduce heat loss within the experimental setup. A schematic representation of the experimental setup is shown in Fig. 2. Temperatures within and outside the cavity were measured using T-type thermocouples (Omega Engineering Inc., USA; the accuracy of 0.1 °C). The arrangement of the thermocouples (23) within and around the cavity is presented in Fig. 3. Before the initiation of this experiment, the thermocouples were calibrated at a temperature range of 15–50 °C. The uncertainty related to the calibrated thermocouples was 0.16 °C.

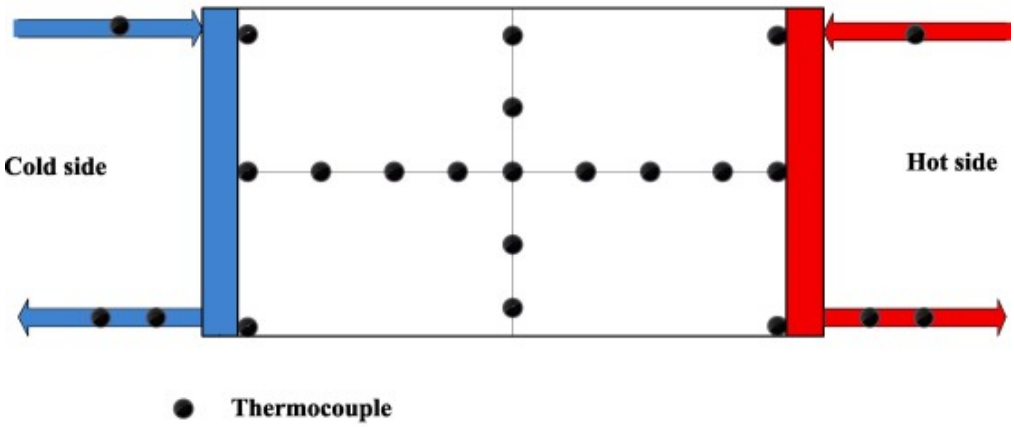

Fig. 3. Thermocouples arrangement.

In this study, a run of four experiments for each sample of DIW and AHFs was carried out at different temperature gradients after charging the cavity with the test samples. Data acquisition of the temperatures and flow rates commenced after the samples have reached a steady-state (after 50 min of charging the cavity with the test sample). The data were logged into a computer (installed with a LABVIEW® software (2014 version)) using a 32-channel data logger (National Instrument; SCXI-1303). Flow rates of the thermal baths were adjusted (within a maximum difference of 4%) to attain thermal equality between both ends of the cavity containing the test samples.

To investigate the effect of magnetic excitation on the convective heat transfer of AHF in the cavity, the AHF sample with the highest heat transfer performance was selected. Two identical electromagnets were mounted on the various walls (top, bottom, and side) of the cavity (containing the selected sample), to impose magnetic excitation of 118.4 G on the sample. These electromagnets were connected to a DC power supply (NIE, model: PS3020 with maximum 20 A and 30 V) to generate magnetic excitation. Increasing the current supply to the electromagnets was noticed to increase the magnetic excitation. A gaussmeter (5180 model, F.W.BELL, USA, 1 G–30 kG with 1.1% accuracy) was used to measure the intensity of the magnetic excitation. The arrangement of the electromagnets is presented in Fig. 4. It should be noted that at the top of the cavity, the electromagnets were placed parallel and perpendicular to the direction of the temperature gradient, whereas, for the sidewall, the electromagnets were positioned both horizontally and vertically. For the bottom wall, the magnets were placed perpendicular to the direction of the temperature gradient. The magnetic excitation was imposed on the cavity walls for 10 min to allow sufficient time for the saturation of the magnetic excitation within the enclosure. On identifying the electromagnets' arrangement with the highest heat transfer enhancement, the magnetic excitation was increased from 48.9 to 219.5 G to investigate the possible augmentation in heat transfer performance.

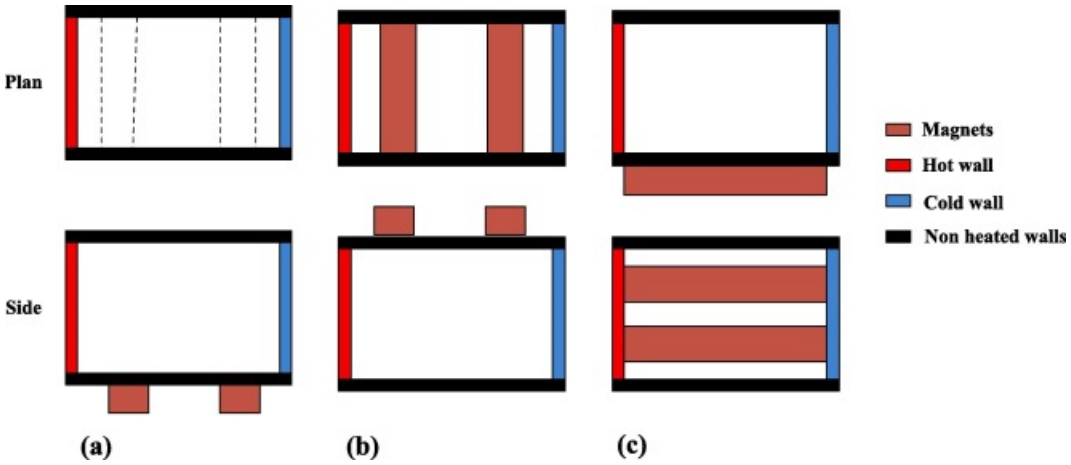

Fig. 4. Positioning of electromagnets on cavity walls; (a) bottom, (b) top, and (c) side.

2.3. Determination of thermophysical properties

The thermal conductivity and viscosity of the AHF for 0.05 vol%–0.3 vol% at a temperature range of 20–40 °C were measured using vibro-viscometer (SV-10, A&D, Japan, ±3% accuracy) and TEMPOS thermal properties analyzer (METER Group; ±10% accuracy for $\varkappa$ = 0.2–2.0 W/m K), respectively. The comparison of the measured thermal conductivity of AHF to that estimated based on modified Maxwell model [37] for hybrid nanofluid was also performed. The thermal expansion coefficient, specific heat capacity, and density of DIW and AHFs were not determined experimentally but by numerical evaluation. As provided in the literature [37], the empirical mixture models for these properties have been modified for hybrid nanofluids, and it was used for the AHF in this study. These properties are given in Eqs. (2), (3), (4), (5).

$$\frac{k_{AHF}}{k_{DIW}} = ((k_{Fe_2O_3}X_{Fe_2O_3} + k_{Al_2O_3}X_{Al_2O_3}) + 2k_{DIW} + 2(\varphi_{Fe_2O_3}k_{Fe_2O_3}X_{Fe_2O_3} + \varphi_{Al_2O_3}k_{Al_2O_3}X_{Al_2O_3}) - 2\varphi_{AHF}k_{DIW}) \times ((k_{Fe_2O_3}X_{Fe_2O_3} + k_{Al_2O_3}X_{Al_2O_3}) + 2k_{DIW} - (\varphi_{Fe_2O_3}k_{Fe_2O_3}X_{Fe_2O_3} + \varphi_{Al_2O_3}k_{Al_2O_3}X_{Al_2O_3}) + \varphi_{AHF}k_{DIW})^{-1} \quad (2)$$

$$\rho_{AHF} = \varphi_{Fe_2O_3}\rho_{Fe_2O_3} + \varphi_{Al_2O_3}\rho_{Al_2O_3} + (1-\varphi_{AHF})\rho_{DIW} \quad (3)$$

$$(\rho\beta)_{AHF} = \varphi_{Fe_2O_3}(\rho\beta)_{Fe_2O_3} + \varphi_{AL_2O_3}(\rho\beta)_{Al_2O_3} + (1-\varphi_{AHF})(\rho\beta)_{DIW} \quad (4)$$

$$(\rho C_p)_{AHF} = \varphi_{Fe_2O_3}(\rho C_p)_{Fe_2O_3} + \varphi_{Al_2O_3}(\rho C_p)_{Al_2O_3} + (1-\varphi_{AHF})(\rho C_p)_{DIW} \quad (5)$$

The correlation developed (from the measured thermophysical properties in this present study) for the viscosity and thermal conductivity of AHF (Fe_2O_3- Al_2O_3/DIW nanofluid) was engaged in the data reduction process.

2.4. Data reduction

To reduce the data of temperatures and flow rates obtained in this study, the thermophysical properties of the test samples of DIW and AHFs were employed in estimating the important variables of Nu, h, $\dot{Q}$, and Ra. $\dot{Q}_{av}$, h_{av}, Nu_{av} and Ra were calculated using Eqs. (5), (6), respectively. The thermal equilibrium reached between the thermal baths and the cavity samples was quantified using Eq. (6).

$$\dot{Q}_{av(samples)}\ (W) = \dot{m}_w C_{p(w)} \Delta T \tag{6}$$

$$\Delta T = \left(T_i - \left(\frac{T_{o,1}+T_{o,2}}{2}\right)\right)_h = \left(\left(\frac{T_{o,1}+T_{o,2}}{2}\right)+T_i\right)_c$$

To obtain averages of

, and related to the free convection of DIW and AHFs in the cavity, Eqs. (7), (8), (9) were used to estimate these variables

$$h_{av} = \frac{\dot{Q}_{av}}{A(T_h - T_c)} \tag{7}$$

$$Ra_{av} = \frac{g\beta(T_h - T_c)(\rho)^2(C_p)L^3}{\mu\kappa} \tag{8}$$

$$Nu_{av} = \frac{hL}{\kappa} \tag{9}$$

2.5. Validation of cavity

Validation of the cavity was carried out by comparing

data of DIW obtained in this work with those of *Nu* data estimated using empirical models sourced from the literature. The models proposed by Berkovsky and Polevikov [30], Leong et al. [38] and Cioni et al. [9] for the prediction of *Nu* of water in a cavity are expressed in Eqs. (10), (11), (12), respectively. Values of *Ra* and *Pr* for DIW and EG-DIW were substituted into Eqs. (10), (11), (12) to obtained *Nu*.

$$Nu = 0.18\left(\frac{Pr}{0.2+Pr}Ra\right)^{0.29}\ (\mathrm{Pr} \le 10^5; Ra \le 10^{10}; 1 \le H/L \le 10) \tag{10}$$

$$Pr = \frac{\mu C_p}{k}$$

$$Nu = 0.08461 Ra^{0.3125}\ (10^4 < Ra < 10^8) \tag{11}$$

$$Nu = 0.145 Ra^{0.292}\ (3.7x10^8 \le Ra \le 7x10^9) \tag{12}$$

2.6. Uncertainty analysis

An analysis of the uncertainty associated with different variables considered in this work was carried out. The purpose was to have a good knowledge of the degree of reliability of the collected data involving these variables. Data of temperatures and flow rates noticed as the main error sources have been propagated using Eqs. (7), (8), (9).

$$\delta\dot{Q} = \left(\left(\frac{\partial\dot{Q}}{\partial\dot{m}}\delta\dot{m}\right)^2 + \left(\frac{\partial\dot{Q}}{\partial C_{p_{DIW}}}\delta C_{p_{DIW}}\right)^2 + \left(\frac{\partial\dot{Q}}{\partial\Delta T}\delta\Delta T\right)^2\right)^{\frac{1}{2}} \tag{13}$$

$$\delta h = \left(\left(\frac{\partial h}{\partial Q}\delta\dot{Q}\right)^2 + \left(\frac{\partial h}{\partial A}\delta A\right)^2 + \left(\frac{\partial h}{\partial T_h}\delta T_h\right)^2 + \left(\frac{\partial h}{\partial T_c}\delta T_c\right)^2\right)^{\frac{1}{2}} \tag{14}$$

$$\delta Nu = \left(\left(\frac{\partial Nu}{\partial h}\delta h\right)^2 + \left(\frac{\partial\dot{Q}}{\partial L}\delta L\right)^2 + \left(\frac{\partial\dot{Q}}{\partial\kappa}\delta\kappa\right)^2\right)^{\frac{1}{2}} \tag{15}$$

The estimated uncertainties were 8.12% ($\dot{Q}$), 3.06% (Nu), and 6.10% (h).

3. Results and discussion

3.1. Morphology and stability of aqueous hybrid ferrofluid

Fig. 5 shows the TEM image of Fe_2O_3-Al_2O_3/DIW nanofluid for φ = 0.3 vol%. A good dispersion of both types of nanoparticles into DIW was noticed in Fig. 5, which indicated good stability of the AHF. The distribution of the hybrid nanoparticles observed in Fig. 5 also reflected the percent weights that were used in the formulation of 0.3 vol% AHF. Both nanoparticles were noticed to be spherical but with the difference in appearance as indicated. Particle size ranges of 20.50 nm–34.99 nm and 16.60 nm–35.31 nm were identified (using TEM) for Al_2O_3 and Fe_2O_3 nanoparticles, respectively. The UV–visible spectrophotometer was used to monitor the AHFs for a duration of 50 h. The stability of the AHF for 0.05, 0.1 and 0.3 vol% is displayed in Fig. 6. For the stability of each AHF monitored, absorbance values of approximately 2.4, 2.5, and 2.8 at wavelengths 297, 299, and 299 nm were recorded for 0.05, 0.1 and 0.3 vol%, respectively. With a wavelength of 225 nm reported for water-based Al_2O_3 nanofluid [9], the wavelength values obtained for the AHF can be connected to the hybridization of Al_2O_3 and Fe_2O_3 nanoparticles. The linearity of the absorbances of AHFs as illustrated in Fig. 6 showed the degree of stability of the nanofluids over time. It is worth noting that the stability reported above was carried out immediately the AHFs were charged into the cavity to check their stability throughout the duration of the experiment and beyond. The AHFs were visually inspected and found to be stable for over one month with little or no sedimentation.

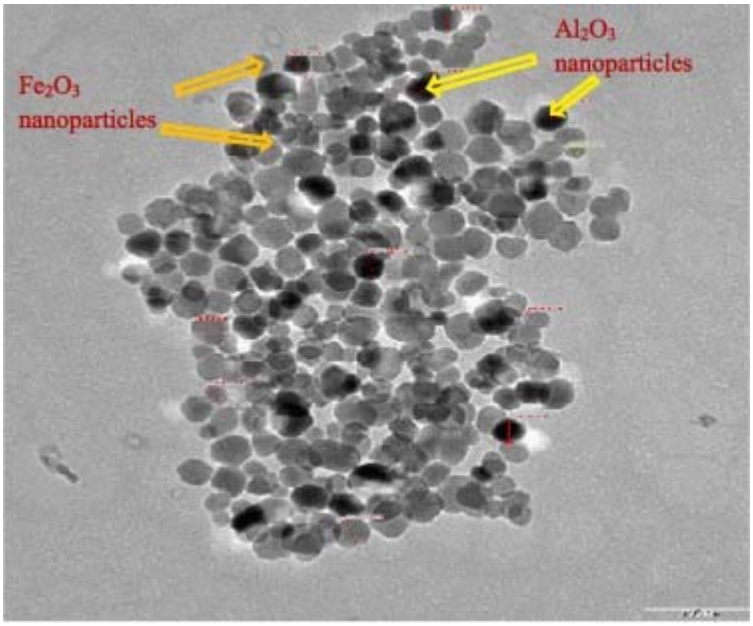

Fig. 5. TEM image of aqueous hybrid ferrofluid (Fe_2O_3- Al_2O_3 (75%:25%)).

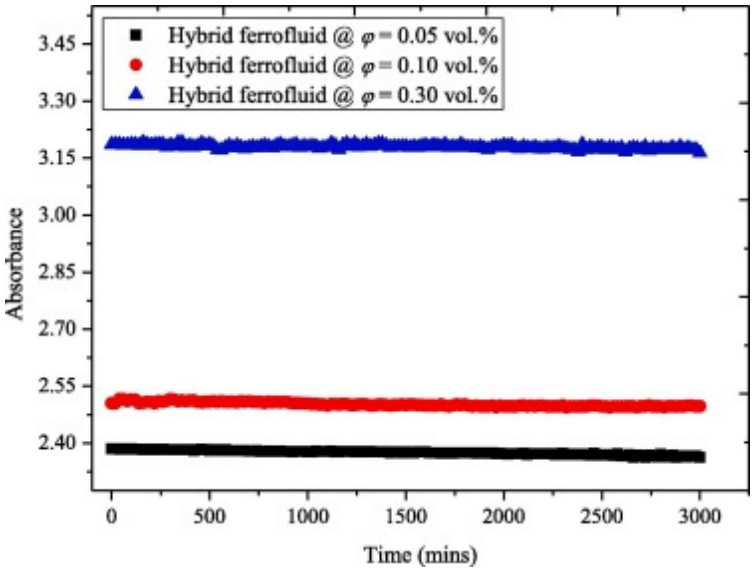

Fig. 6. Stability of different concentrations of aqueous hybrid ferrofluid.

3.2. Measured thermophysical properties aqueous hybrid ferrofluids

A plot of the effective viscosity of AHFs against temperature for various volume concentrations is presented in Fig. 7. It was observed that the effective viscosity of AHFs was enhanced as the volume concentration increased. Also, this thermal property detracted as the temperature appreciated. The obtained result was observed to agree with the report found in the literature concerning the effect of φ and temperature on the effective viscosity of nanofluid [39], [40], [41]. Enhancement range of 4.55–20.43% was recorded for the AHF in comparison with the DIW. A new correlation which depended on φ and temperature has been developed for predicting the effective viscosity of AHF based on the measured data. The developed correlation was expressed in Equation (16) and it has a prediction accuracy of 98% with a margin of deviation of −2.34% and 2.30%. The AHF was found to have a lower viscosity in relation to the Fe_2O_3-DIW nanofluid as published by Joubert et al. [35]. The utilization of 25 wt% Al_2O_3 nanoparticle in AHF was observed to cause a reduction in the viscosity of the mono-particle ferrofluid (Fe_2O_3-DIW). Using the correlation proposed in the work of Joubert et al. [35] and this study (at the temperatures and φ considered in this present work), the viscosity of the mono-particle ferrofluid was estimated to be reduced by 28.02–31.02%. This indicated that the use of AHF resulted in viscosity reduction, which would be beneficial to the convective heat transfer and flow of nanofluids.

$$\mu_{HF} = 1.3291 - 0.0164T + 0.3010\varphi \, (R^2 = 0.962) \tag{16}$$

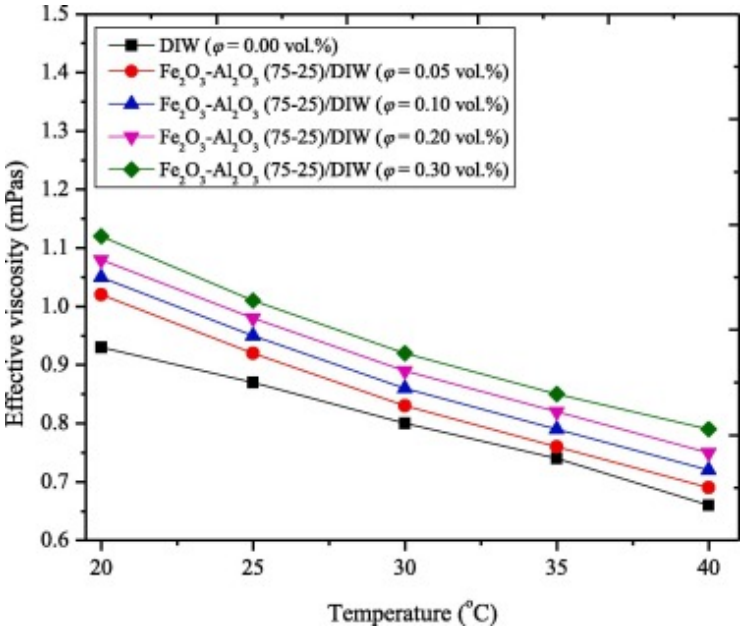

Fig. 7. Effect of temperature on effective viscosity of aqueous hybrid ferrofluid.

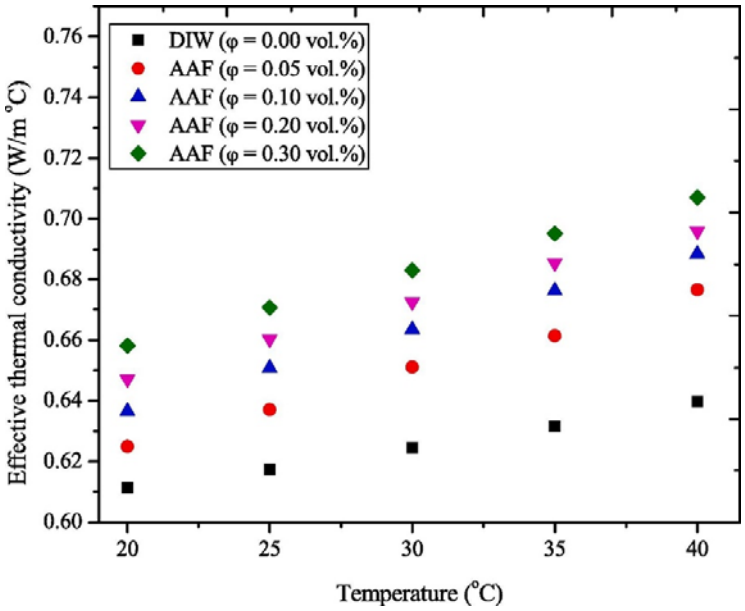

Fig. 8. Effect of temperature on effective thermal conductivity of aqueous hybrid ferrofluid.

In Fig. 8, the influence of φ and temperature on the thermal conductivity of AHF is illustrated. Both temperature and φ were noticed to enhance the effective thermal conductivity of AHF with the temperature being more significant than φ. Besides, the AHFs were observed to have better thermal conductivity than DIW. Since the hybrid nanoparticles have higher thermal conductivity (individually and combined) than DIW, expectedly the dispersion of the nanoparticles into DIW would produce AHFs with higher thermal conductivity. Also, it was estimated that the AHFs have thermal conductivity augmentation of 0.58%–3.32% over that of DIW for the range of φ and temperature studied. A formula was proposed using the experimental data (thermal conductivity) for predicting the AHF thermal conductivity as given in Equation (17). The

formula has a prediction performance of over 98% with a margin of deviation of −4.25% and 3.88%.

$$\kappa_{AHF} = 2.508 \times 10^{-3} T + 0.1220\varphi + 0.5720 \tag{17}$$

Plots of the effective thermal expansion coefficient, density, and specific heat capacity of AHF were presented in Fig. 9, Fig. 10, Fig. 11, respectively. It was observed in these figures that an increase in temperature caused an enhancement of effective thermal expansion coefficient and a depreciation of effective density and specific heat capacity of AHF. Concerning an increase in volume concentration, the effective density was augmented while the specific heat capacity and thermal expansion coefficient were reduced for AHF. These results (for density and specific heat capacity) agreed with previous studies found in the literature for hybrid nanofluids [42], [43]. A comparison of this proposed formula with that of the modified Maxwell model (Eq. (6)) revealed that the latter underestimated the experimental data as presented in Fig. 12. This implied that using theoretical and empirical models could lead to overestimation of resultant output when used in the data reduction process. Thus, it is advisable to determine thermophysical properties engaged in the data reduction process for studies involving natural convection of nanofluids in various enclosures, experimentally. This is consistent with the work of Astanina et al. [44] which showed that the use of various correlations (experimental and theoretical) led to a considerable heat transfer in a partially-heated square cavity containing Al_2O_3/water nanofluid and exposed to an inclined magnetic field.

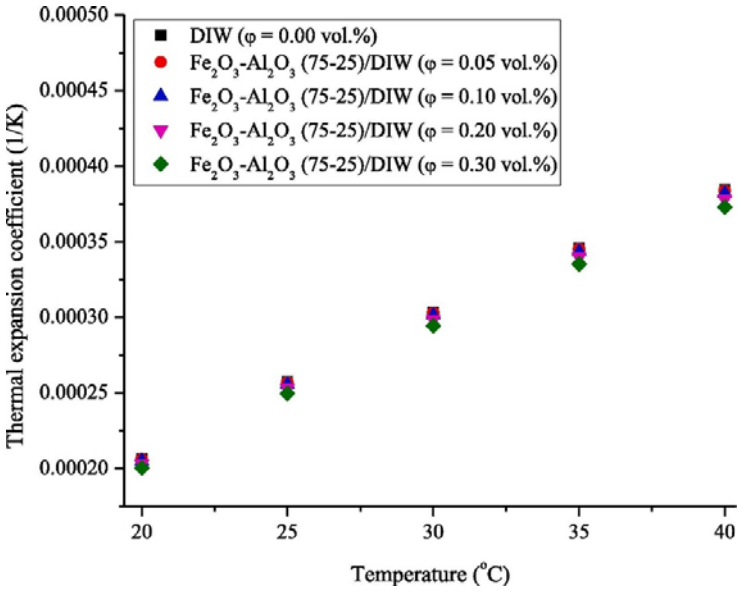

Fig. 9. Estimated effective thermal expansion coefficient of aqueous hybrid ferrofluid.

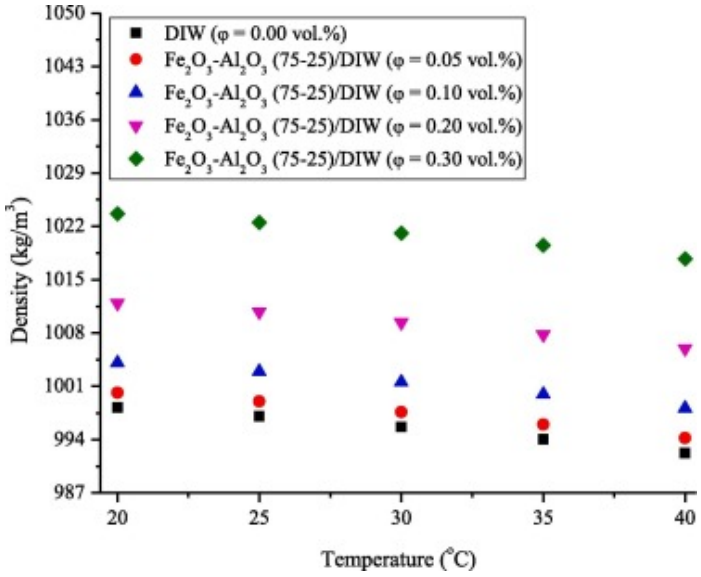

Fig. 10. Estimated effective density of aqueous hybrid ferrofluid.

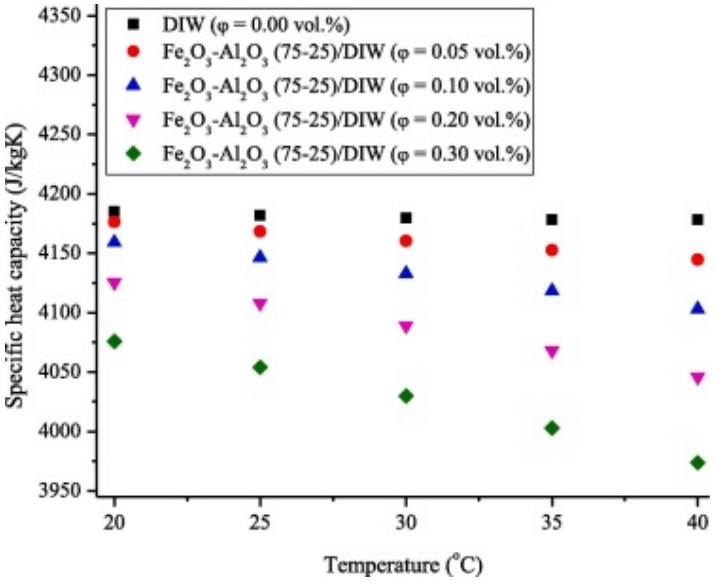

Fig. 11. Estimated effective specific heat capacity of aqueous hybrid ferrofluid.

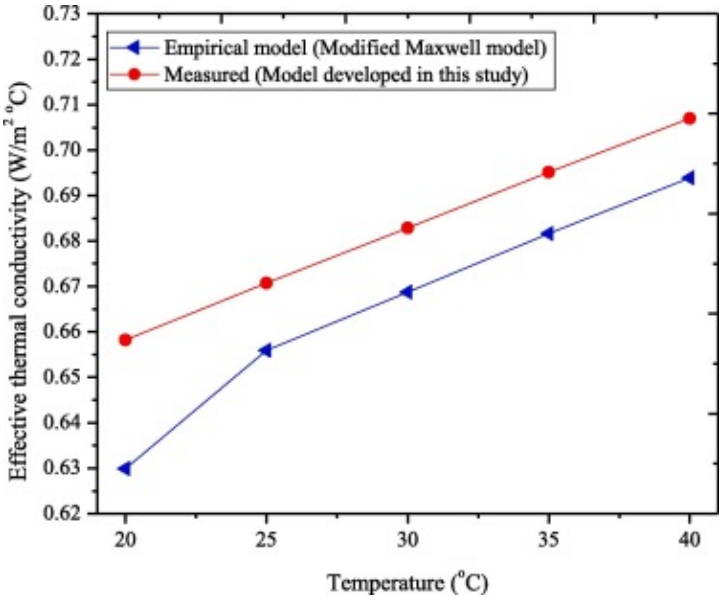

Fig. 12. Comparison of measured and empirically derived effective thermal conductivity of AAF for volume fraction of 0.30 vol%.

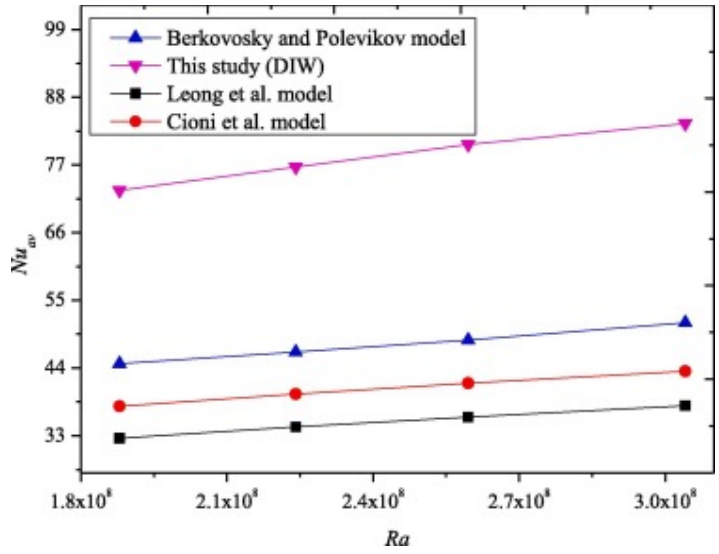

Fig. 13. Cavity validation with empirical models.

3.3. Cavity validation

The validation of the cavity was carried out using the *Nu* data for DIW obtained in this study. To depict the validity of the cavity, a comparison of the *Nu* values obtained in this work with those calculated using existing numerical models reported in the literature for natural convection [9], [38], [45] is plotted in Fig. 13. It was observed that the models could not predict the experimental *Nu* values correctly but rather underestimated it using the *Ra* values (for DIW) obtained in this work. It was clear from the literature that Leong et al. [38] proposed a model having *Ra* range of $10^4 < Ra < 10^8$, which was less than the values ($1.37 \times 10^8 < Ra < 2.20 \times 10^8$) obtained experimentally in this work. On the contrary, the model of Cioni et al. [9] has a *Ra* range ($3.7 \times 10^8 < Ra < 7 \times 10^9$) higher than the experimental *Ra*

range. However, the model proposed by Berkovsky and Polevikov [45] with a range of $Ra \leq 10^{10}$ was well within the range obtained for this study. Conclusively, the experimental values were found to be significantly higher than those estimated by these models (see Fig. 13). Thus, the obtained result agreed with previous studies in the literature that reported that none of these models successively estimated the experimental *Nu* data for DIW in a cavity, though with similar trends [23], [26].

3.4. Heat transfer performance of aqueous hybrid ferrofluids (without magnetic induction)

This present study engaged stable aqueous Fe_2O_3-Al_2O_3 nanofluids (AHFs) formulated for various φ in a rectangular cavity subjected to different ΔT conditions. The thermal transport behaviour of AHFs (in the cavity) was studied for h_{av}, Nu_{av}, and $\dot{Q}_{av}$. The plot of Nu_{av} against *Ra* at different φ is presented in Fig. 14 with *Ra* ranging from 1.49×10^8–3.04×10^8. The DIW has *Ra* range of 1.88×10^8–3.04×10^8 while the AHFs were with a range of 1.49×10^8–2.68×10^8. From Fig. 14, an enhancement in the Nu_{av} was observed with increasing φ, ΔT and *Ra*. Generally, the Nu_{av} of AHFs was higher than that of DIW. The dispersion of hybrid nanoparticles (Fe_2O_3 and Al_2O_3) into the DIW was noticed to cause a decrease in *Ra* at each ΔT (when compared with *Ra* for DIW) with a corresponding increase in the Nu_{av} for the AHF samples. Thus, the *Ra* was directly related to the Nu_{av}. This trend agreed with previous studies [8], [23] and can be ascribed to the difference in the thermophysical properties of the DIW as afforded by the dispersal of hybrid nanoparticles into it (see Fig. 7, Fig. 8). From Fig. 14, 0.1 vol% AHF was noticed to have the highest Nu_{av} (93.26) at $Ra = 2.68 \times 10^8$ and ΔT = 35 °C. This was followed by 0.05 vol%, 0.2 vol%, and 0.3 vol% AHFs and lastly the DIW. The Nu_{av} of 93.26 attained in this present study was slightly higher than the value of 82.76 (at $Ra = 3.94 \times 10^8$ and φ = 0.1 vol%) reported by Joubert et al. [35] on investigating the thermo-convection of aqueous Fe_2O_3 nanofluids in a rectangular enclosure. The formulation of AHFs by adding Al_2O_3 (25%) and Fe_2O_3 nanoparticles (75%) to DIW could be connected to the enhancement observed in this work.

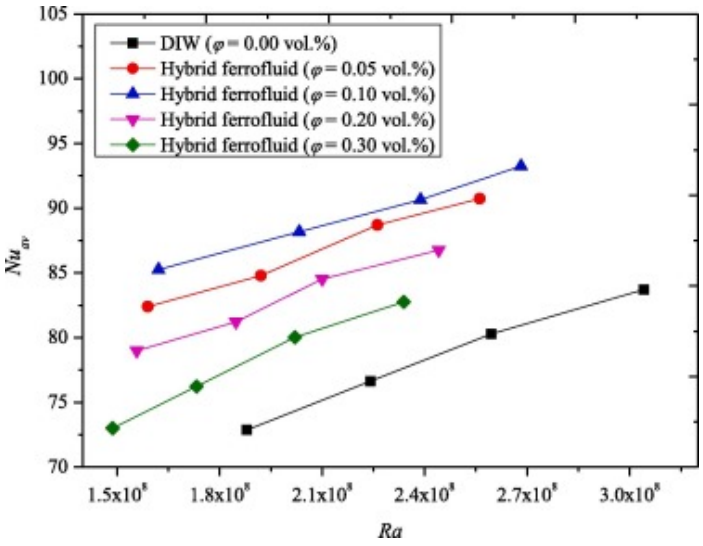

Fig. 14. Effect of *Ra* on Nu_{av} for test samples.

In Fig. 15, the influence of φ and ΔT on the Nu_{av} is presented. The increase in ΔT was observed to have a direct impact on the Nu_{av} by enhancing it, whereas a rise in φ (0.00–0.10 vol%)

augmented the Nu_{av} to a peak, and after that, it diminished (0.10–0.3 vol%.). In relation to the DIW, the Nu_{av} was enhanced by 10.81%, 6.41%, and 3.66% for 0.1 vol% AHF, 0.05 vol% AHF, and 0.2 vol% AHF, respectively, and deteriorated by 1.12% for 0.3 vol% AHF. The optimum augmentation (10.81%) of the Nu_{av} obtained in this work was slightly higher than the value of 5.63% published by Joubert et al. [35]. This clearly showed the possible enhancement in heat transfer that can be provided when hybrid nanofluids are engaged in thermo-convection studies. Based on the findings (from Fig. 7) that the effective viscosity of AHF was enhanced with increasing value of φ, the buoyancy force within the cavity was suppressed at higher concentrations of the hybrid nanoparticles due to increased viscosity. This scenario led to deduction in the Nu_{av} after a peak has been reached. Though the effective thermal conductivity was augmented with increasing φ (see Fig. 8), the enhancement in the viscosity of AHF at high φ caused the convective flow of AHF in the cavity to diminish. Thus, the deterioration of the Nu_{av}, as an increase in φ would further enhance the viscosity of AHF.

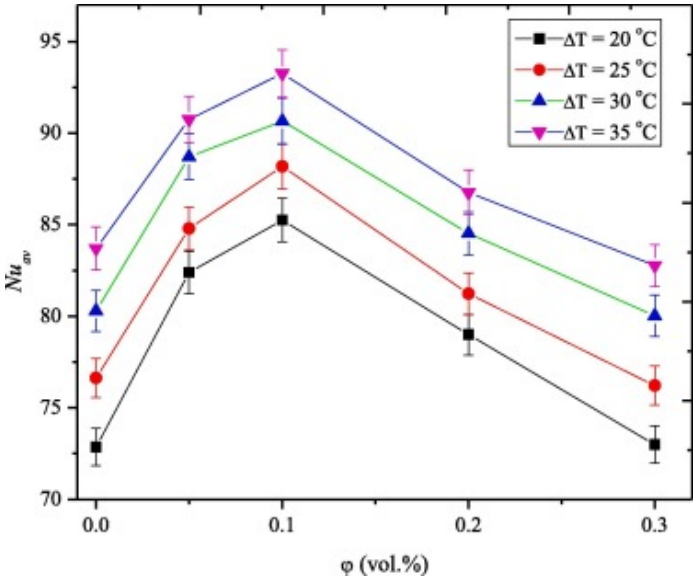

Fig. 15. Effect of volume fraction on Nu_{av} for test samples.

A formula was developed from the Nu_{av} data of AHF, and it was expressed in Eq. (18). The prediction performance of the formula was 94%.

$$Nu = 0.721(Ra)^{0.2429} 9\varphi^{-0.0613} \ (R^2 = 93.85\%) \tag{18}$$

The relationship between the predicted and experimental Nu_{av} values is presented in Fig. 16. The formula proposed can predict the experimental values with a margin of deviation of −2.66% and 2.96% and an average absolute deviation of 1.498%.

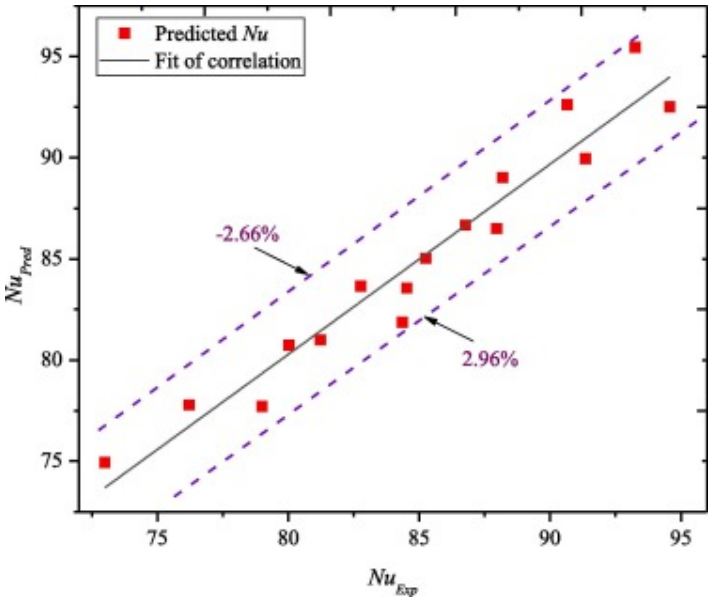

Fig. 16. Fit of the proposed formula for predicting *Nu*.

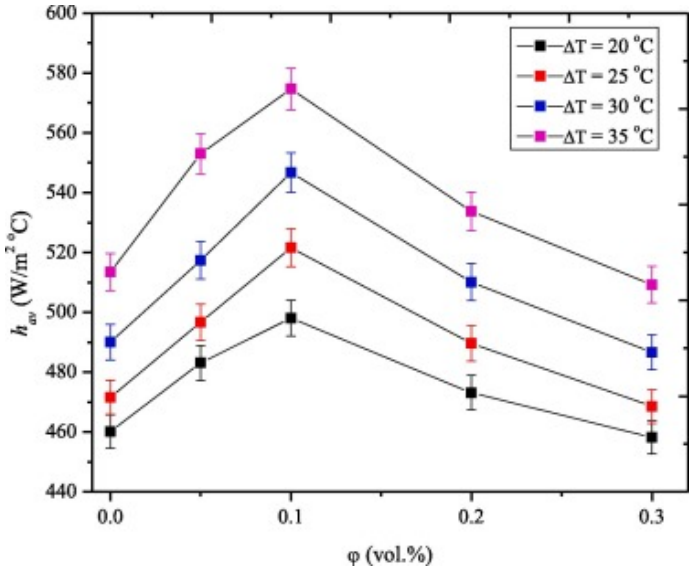

Fig. 17. Effect of volume fraction on h_{av} for test samples.

In Fig. 17, the influence of φ on the h_{av} at various ΔT for all test samples is presented. Expectedly, the h_{av} was enhanced with increasing ΔT for all the samples considered in this work. However, this was not the case when φ was increased from 0.0 to 0.3 vol%. The numerical value of the h_{av} for DIW (φ = 0.00 vol%) was observed to be improved with increasing φ for 0.05–0.2 vol% AHFs and it slightly deteriorated for 0.3 vol% AHF. A peak in the h_{av} (574.66 W/m^2 °C) was achieved using 0.1 vol% AHF at ΔT = 35 °C and this corresponded to 11.92% enhancement relative to the h_{av} of DIW. For 0.05 vol% and 0.2 vol% AHFs, the h_{av} was enhanced by 7.69% and 3.95%, respectively, and for 0.3 vol% AHF, an attenuation of h_{av} by 0.8% were observed in comparison to the h_{av} of DIW at ΔT = 35 °C. The decline in the augmentation of h_{av} for 0.20 vol% and the subsequent deterioration for 0.30 vol% can be linked to the increase in their viscosity at these concentrations, which retarded the convective heat

transfer in the cavity and consequently caused the reduction of h_{av} for these AHF samples. With previous studies reporting h_{av} of 15% [9] and 18% [21] for alumina nanofluids and 12.7–19.4% [31] for Al_2O_3-MWCNT/water nanofluids in square cavities, the value of h_{av} obtained for AHF was found to be in close agreement with these publications.

To understand the free convection thermal transport capability of AHFs in the cavity, the $\dot{Q}_{av}$ as a function of φ at different ΔT was examined. As shown in Fig. 18, an increase in ΔT from 20 to 35 °C was noticed to produce a corresponding increase in $\dot{Q}_{av}$ for all the studied samples. Increased agitation of molecules of the samples in the cavity due to ΔT increase was responsible for the improvement in $\dot{Q}_{av}$. The dispersion of hybrid nanoparticles into DIW was noticed to enhance $\dot{Q}_{av}$ for 0.05–0.2 vol% AHFs with the peak augmentation recorded for 0.1 vol% AHF. However, a deterioration was observed for 0.3 vol% AHF. In relation to $\dot{Q}_{av}$ for DIW, the AHF samples of 0.05 vol%, 0.1 vol%, and 0.2 vol% showed enhancement of $\dot{Q}_{av}$ by 8.45%, 10.79%, and 5.08%, respectively, and depreciation of 3.01% for 0.3 vol% AHF. Recently, Sharifpur et al. [23] reported heat transfer enhancement of 8.2% using TiO_2/DIW nanofluid in a rectangular cavity while Giwa et al. [31] published 7.2–9.8% as the value for the heat transfer augmentation of Al_2O_3-MWCNT/water nanofluids in a square enclosure. The value of 10.79% achieved for thermal transport enhancement of AHF in this study was noticed to be slightly above those of these previous studies.

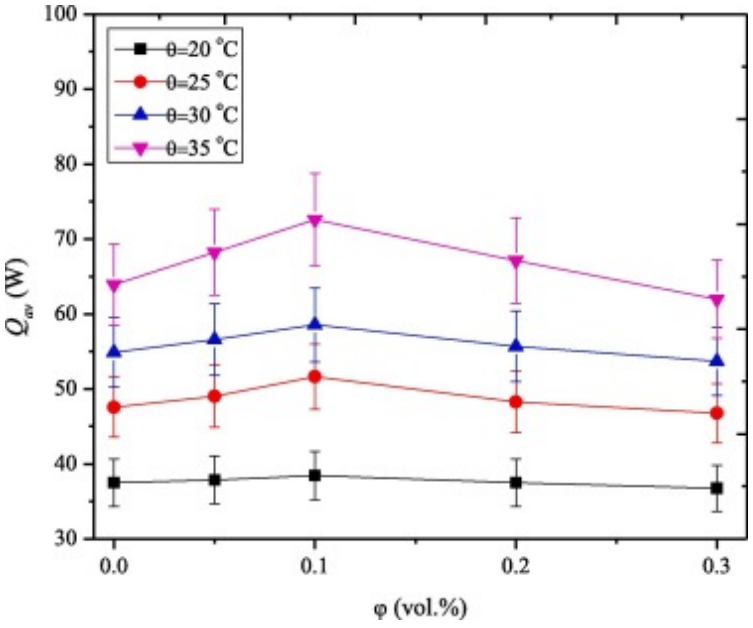

Fig. 18. Effect of volume fraction on h_{av} for test samples.

3.5. Heat transfer performance of aqueous hybrid ferrofluids (with magnetic induction)

Since 0.10 vol% AHF was noticed to offer the maximum heat transfer performance, the impact of external magnetic induction at various parts of the cavity on its free convection heat transfer was investigated. The effect of the magnetic induction of 118.1 G on different walls of the cavity containing 0.1 vol% AHF (as earlier described in sub-Section 2.2) is shown in Fig. 19. Nu_{av} was augmented by 1.83%, 1.31% and 2.64% (at $Ra = 2.01 \times 10^8$) when the magnetic field strength of 118.1 G was induced horizontally on the sidewall, perpendicular to the direction of temperature

gradient on the bottom wall and vertically on the sidewall of the cavity, respectively, relative to the case of Nu_{av} of 0.1 vol% AHF without magnetic induction. The introduction of magnetic fields into the setup was observed to create magnetic forces into the fluid with the evidence of a rise in the temperature of 0.1 vol% AHF, which consequently led to the augmentation of the convective flow within the cavity. Consequently, the h_{av} of 0.1 vol% AHF was enhanced causing Nu_{av} and heat transfer performance ($\dot{Q}_{av}$) augmentation. However, the deterioration of Nu_{av} by 1.11% and 1.64% (relative to Nu_{av} of 0.1 vol% AHF without magnetic induction) was observed with the magnetic induction of 118.1 G parallel and perpendicular to the direction of the temperature gradient on the top wall of the cavity, respectively. Owing to the direction (perpendicular and parallel to temperature gradient) for the top wall, the induced magnetic field was noticed to retard the convective flow due to suppression of buoyancy forces within the cavity.

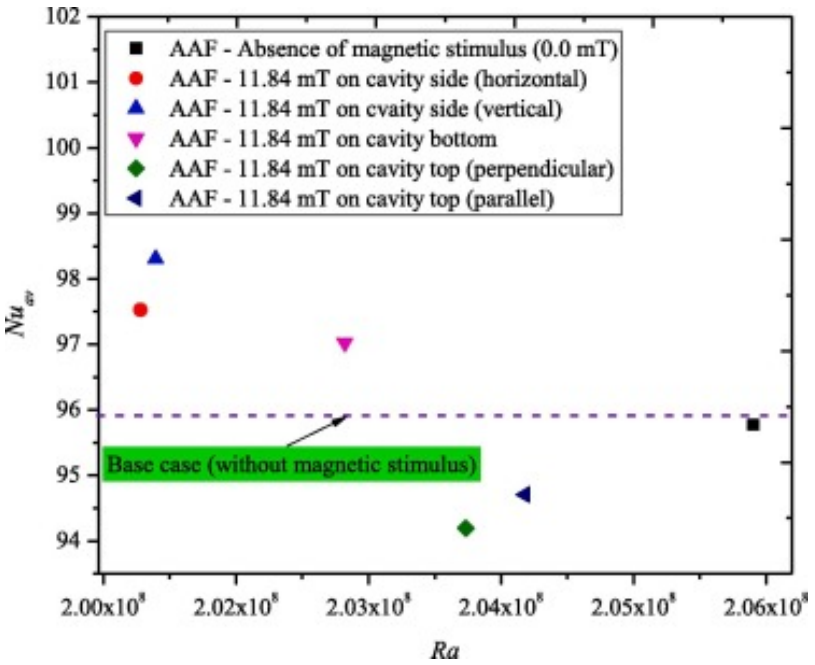

Fig. 19. Effect of magnetic induction on Nu_{av} for different walls of the cavity.

On detecting that the imposition of the magnetic field vertically on the sidewall and perpendicular to the direction of the temperature gradient on the bottom wall caused heat transfer enhancement of 0.1 vol% AHF, the magnetic strength range of 48.9 G–219.5 G was studied to understand how this affected the Nu_{av}. The obtained result is presented in Fig. 20. It can be observed that increasing the magnetic strength from 48.9 G to 219.5 G caused the enhancement of Nu_{av}. With the magnetic induction positioned vertically on the side of the cavity, the Nu_{av} was augmented by 1.39%–4.91% when the magnetic field was increased from 48.9 G to 219.5 G, while the Nu_{av} was improved by 1.06%–2.59% on increasing the magnetic field. In addition, the Nu_{av} was improved by 0.53%–1.75% when the magnetic fields were induced perpendicular to the direction of the temperature gradient on the bottom wall subject to the increase in magnetic field strength (Fig. 20). This showed that the vertical positioning of the electromagnets to induce magnetic fields on the side of the rectangular cavity afforded the maximum Nu_{av} enhancement with the peak obtained at 219.5 G. For this magnetic induction position, maximum augmentation of 5.38% and 4.31% were estimated for h_{av} and $\dot{Q}_{av}$ at 219.5 G, respectively. The published works of Joubert et al. [35], Yamagushi et al. [34] and Roszko, and

Fornalik-Wajs [13] agreed with this outcome that increasing the strength of magnetic fields induced on the walls of cavities containing nanofluids resulted in the augmentation of heat transfer performance. With Joubert et al. [35], the exposure of permanent magnets of 700 G to the top and bottom walls (at the hot side) of a rectangular cavity containing Fe_2O_3/DIW nanofluid (φ = 0.10 vol%) enhanced Nu_{av} by 2.81% above that of the case without magnet induction. It can be concluded that the vertical positioning of the induced magnetic fields provided the maximum heat transfer enhancement of all the electromagnets' arrangements considered in this present study.

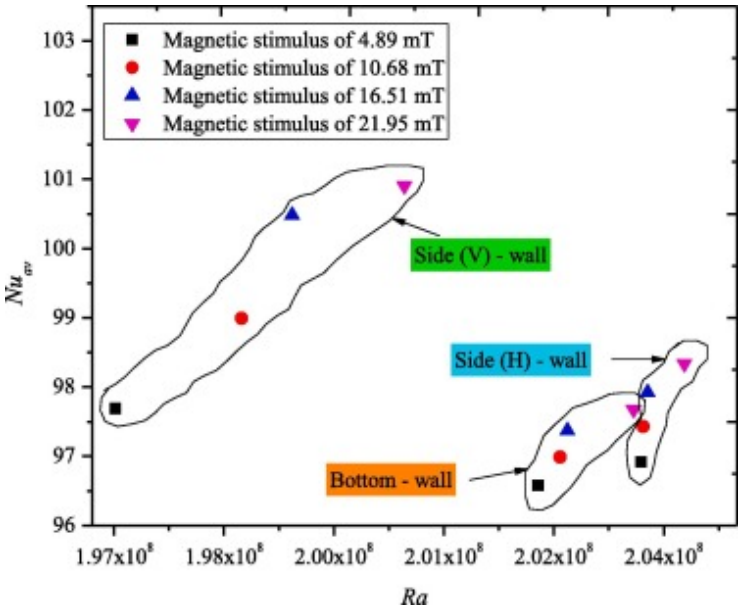

Fig. 20. Nu_{av} enhancement with increasing magnetic induction.

4. Conclusion

Stable AHFs (0.05–0.3 vol%) were formulated, and the thermal properties (thermal conductivity and viscosity) were measured at temperatures of 20–40 °C. With the AHFs charged into a rectangular cavity, an examination of the free convection heat transfer performance was conducted at a steady-state under varying temperature gradients with and without a magnetic induction. Without magnetic induction on the cavity walls, improvements in h_{av}, Nu_{av}, and $\dot{Q}_{av\ av}$ were observed for 0.05–0.2 vol% AHFs in comparison with the DIW. Peak heat transfer enhancement of 10.81% was achieved using 0.10 vol% AHF at ΔT = 35 °C. By inducing magnetic fields vertically on the side wall of the cavity, maximum enhancement of Nu_{av} was achieved compared to other magnetic induction arrangements. Additionally, increasing the magnetic field strength (48.9–219.5 G) was noticed to further enhance heat transfer of 0.10 vol% AHF contained in the cavity. The use of hybrid nanofluid was revealed to have better heat transfer performance than mono-particle nanofluids. Moreso, the imposition of the magnetic field on 0.1 vol% AHF has been demonstrated to improve heat transfer.

Declaration of Competing Interest

The authors declare that they have no known competing financial interests or personal relationships that could have appeared to influence the work reported in this paper.

Acknowledgement

The funding for this study is provided by the National Research Foundation of South Africa under the Renewable and Sustainable Energy Doctoral Scholarships.

References

[1] F. Selimefendigil, H.F. Öztop, Conjugate natural convection in a nanofluid filled partitioned horizontal annulus formed by two isothermal cylinder surfaces under magnetic field, *Int. J. Heat Mass Transf.* 108 (2017) 156–171, https://doi.org/10.1016/j.ijheatmasstransfer.2016.11.080.
[2] Z. Haddad, H.F. Oztop, E. Abu-Nada, A. Mataoui, A review on natural convective heat transfer of nanofluids, *Renew. Sustain. Energy Rev.* 16 (2012) 5363–5378, https://doi.org/10.1016/j.rser.2012.04.003.
[3] S. Mojumder, K.M. Rabbi, S. Saha, M.N. Hasan, S.C. Saha, Magnetic field effect on natural convection and entropy generation in a half-moon shaped cavity with semi-circular bottom heater having different ferrofluid inside, *J. Magn. Magn. Mater.* 407 (2016) 412–424, https://doi.org/10.1016/j.jmmm.2016.01.046.
[4] M. Leporini, F. Corvaro, B. Marchetti, F. Polonara, M. Benucci, Experimental and numerical investigation of natural convection in tilted square cavity filled with air, *Exp. Therm. Fluid Sci.* 99 (2018) 572–583, https://doi.org/10.1016/j.expthermflusci.2018.08.023.
[5] F. Corvaro, G. Nardini, M. Paroncini, R. Vitali, Piv and numerical analysis of natural convective heat transfer and fluid flow in a square cavity with two vertical obstacles, *Int. J. Heat Technol.* 33 (2015) 51–56, https://doi.org/10.18280/ijht.330208.
[6] M.H. Esfe, A.A.A. Arani, W.-M. Yan, A. Aghaei, Natural convection in T-shaped cavities filled with water-based suspensions of COOH-functionalized multi walled carbon nanotubes, *Int. J. Mech. Sci.* 121 (2017) 21–32, https://doi.org/10.1016/j.ijmecsci.2016.12.011.
[7] C.C. Liao, Heat transfer transitions of natural convection flows in a differentially heated square enclosure filled with nanofluids, *Int. J. Heat Mass Transf.* 115 (2017) 625–634, https://doi.org/10.1016/j.ijheatmasstransfer.2017.08.045.
[8] P.S. Joshi, A. Pattamatta, Buoyancy induced convective heat transfer in particle, tubular and flake type of nanoparticle suspensions, *Int. J. Therm. Sci.* 122 (2017) 1–11, https://doi.org/10.1016/j.ijthermalsci.2017.07.030.
[9] H. Ghodsinezhad, M. Sharifpur, J.P. Meyer, Experimental investigation on cavity flow natural convection of Al2O3–water nanofluids, *Int. Commun. Heat Mass Transf.* 76 (2016) 316–324, https://doi.org/10.1016/j.icheatmasstransfer.2016.06.005.
[10] Z. Li, M. Sheikholeslami, A.J. Chamkha, Z.A. Raizah, S. Saleem, Control volume finite element method for nanofluid MHD natural convective flow inside a sinusoidal annulus under the impact of thermal radiation, *Comput. Methods Appl. Mech. Eng.* 338 (2018) 618–633, https://doi.org/10.1016/j.cma.2018.04.023.
[11] I. Jelodari, A.H. Nikseresht, Effects of Lorentz force and induced electrical field on the thermal performance of a magnetic nanofluid-filled cubic cavity, *J. Mol. Liq.* 252 (2018) 296–310, https://doi.org/10.1016/j.molliq.2017.12.143.
[12] H. Yamaguchi, X.R. Zhang, X.D. Niu, K. Yoshikawa, Thermomagnetic natural convection of thermo-sensitive magnetic fluids in cubic cavity with heat generating object inside, *J. Magn. Magn. Mater.* 322 (2010) 698–704, https://doi.org/10.1016/j.jmmm.2009.10.044.
[13] A. Roszko, E. Fornalik-Wajs, Extend of magnetic field interference in the natural convection of diamagnetic nanofluid, *Heat Mass Transf, Und Stoffuebertragung.* (2017) 1–12, https://doi.org/10.1007/s00231-017-2172-7.
[14] K.S. Suganthi, K.S. Rajan, Metal oxide nanofluids: Review of formulation, thermo-physical properties, mechanisms, and heat transfer performance, *Renew. Sustain. Energy Rev.* 76 (2017) 226–255, https://doi.org/10.1016/j.rser.2017.03.043.

[15] N. Putra, W. Roetzel, S.K. Das, Natural convection of nano-fluids, *Heat Mass Transf. Und Stoffuebertragung*. 39 (2003) 775–784, https://doi.org/10.1007/s00231-002-0382-z.
[16] H. Li, Y. He, Y. Hu, B. Jiang, Y. Huang, Thermophysical and natural convection characteristics of ethylene glycol and water mixture based ZnO nanofluids, *Int. J. Heat Mass Transf.* 91 (2015) 385–389, https://doi.org/10.1016/j.ijheatmasstransfer.2015.07.126.
[17] Y. Hu, Y. He, S. Wang, Q. Wang, H.I. Schlaberg, Experimental and Numerical Investigation on Natural Convection Heat Transfer of TiO2-Water Nanofluids in a Square Enclosure, *J. Heat Transfer*. 136 (2014) 022502, , https://doi.org/10.1115/1.4025499.
[18] K. Kouloulias, A. Sergis, Y. Hardalupas, Sedimentation in nanofluids during a natural convection experiment, *Int. J. Heat Mass Transf.* 101 (2016) 1193–1203, https://doi.org/10.1016/j.ijheatmasstransfer.2016.05.113.
[19] M. Torki, N. Etesami, Experimental investigation of natural convection heat transfer of SiO2/water nanofluid inside inclined enclosure, *J. Therm. Anal. Calorim.* 9 (2019), https://doi.org/10.1007/s10973-019-08445-9.
[20] I.D. Garbadeen, M. Sharifpur, J.M. Slabber, J.P. Meyer, Experimental study on natural convection of MWCNT-water nanofluids in a square enclosure, *Int. Commun. Heat Mass Transf.* 88 (2017) 1–8, https://doi.org/10.1016/j.icheatmasstransfer.2017.07.019.
[21] C.J. Ho, W.K. Liu, Y.S. Chang, C.C. Lin, Natural convection heat transfer of alumina-water nanofluid in vertical square enclosures: An experimental study, *Int. J. Therm. Sci.* 49 (2010) 1345–1353, https://doi.org/10.1016/j.ijthermalsci.2010.02.013.
[22] A.G.A. Nnanna, Experimental Model of Temperature-Driven Nanofluid, *J. Heat Transfer*. 129 (2007) 697, https://doi.org/10.1115/1.2717239.
[23] M. Sharifpur, A.B. Solomon, T.L. Ottermann, J.P. Meyer, Optimum concentration of nanofluids for heat transfer enhancement under cavity flow natural convection with TiO2–water, *Int. Commun. Heat Mass Transf.* 98 (2018) 297–303, https://doi.org/10.1016/j.icheatmasstransfer.2018.09.010.
[24] M.R. Khadangi Mahrood, S.G. Etemad, R. Bagheri, Free convection heat transfer of non Newtonian nanofluids under constant heat flux condition, *Int. Commun. Heat Mass Transf.* 38 (2011) 1449–1454. doi:10.1016/j.icheatmasstransfer.2011.08.012.
[25] R. Choudhary, S. Subudhi, Aspect ratio dependence of turbulent natural convection in Al2O3/water nanofluids, *Appl. Therm. Eng.* 108 (2016) 1095–1104, https://doi.org/10.1016/j.applthermaleng.2016.08.016.
[26] A. Brusly Solomon, J. van Rooyen, M. Rencken, M. Sharifpur, J.P. Meyer, Experimental study on the influence of the aspect ratio of square cavity on natural convection heat transfer with Al2O3/water nanofluids, *Int. Commun. Heat Mass Transf.* 88 (2017) 254–261, https://doi.org/10.1016/j.icheatmasstransfer.2017.09.007.
[27] M. Ali, O. Zeitoun, S. Almotairi, H. Al-Ansary, The effect of alumina–water nanofluid on natural convection heat transfer inside vertical circular enclosures heated from above, *Heat Transf. Eng.* 34 (2013) 1289–1299, https://doi.org/10.1080/01457632.2013.793115.
[28] M. Ali, O. Zeitoun, S. Almotairi, Natural convection heat transfer inside vertical circular enclosure filled with water-based Al2O3 nanofluids, *Int. J. Therm. Sci.* 63 (2013) 115–124, https://doi.org/10.1016/j.ijthermalsci.2012.07.008.
[29] H. Moradi, B. Bazooyar, A. Moheb, S.G. Etemad, Optimization of natural convection heat transfer of Newtonian nanofluids in a cylindrical enclosure, *Chinese J. Chem. Eng.* 23 (2015) 1266–1274, https://doi.org/10.1016/j.cjche.2015.04.002.
[30] A. Brusly Solomon, M. Sharifpur, T. Ottermann, C. Grobler, M. Joubert, J.P. Meyer, Natural convection enhancement in a porous cavity with Al2O3-Ethylene glycol/water nanofluids, *Int. J. Heat Mass Transf.* 108 (2017) 1324–1334, https://doi.org/10.1016/j.ijheatmasstransfer.2017.01.009.
[31] S.O. Giwa, M. Sharifpur, J.P. Meyer, Heat transfer enhancement of dilute Al2O3-MWCNT water based hybrid nanofluids in a square cavity, in: *Int. Heat Transf. Conf.,* 2018: pp. 5365–5372.

doi:10.1615/ihtc16.hte.023927.
[32] S.O. Giwa, M. Sharifpur, J.P. Meyer, Experimental study of thermo-convection performance of hybrid nanofluids of Al2O3-MWCNT / water in a differentially heated square cavity, *Int. J. Heat Mass Transf.* 119072 (2019), https://doi.org/10.1016/j.ijheatmasstransfer.2019.119072.
[33] A.B. Solomon, M. Sharifpur, J.P. Meyer, J.S. Ibrahim, B. Immanuel, Convection heat transfer with water based mango bark nanofluids, in: *13th Int. Conf. Heat Transf. Fluid Mech. Thermodyn.*, Portorož, Slovenia, 2017.
[34] H. Yamaguchi, X.-D. Niu, X.-R. Zhang, K. Yoshikawa, Experimental and numerical investigation of natural convection of magnetic fluids in a cubic cavity, *J. Magn. Magn. Mater.* 321 (2009) 3665–3670, https://doi.org/10.1016/j.jmmm.2009.07.013.
[35] J.C. Joubert, M. Sharifpur, A.B. Solomon, J.P. Meyer, Enhancement in heat transfer of a ferrofluid in a differentially heated square cavity through the use of permanent magnets, *J. Magn. Magn. Mater.* 443 (2017) 149–158, https://doi.org/10.1016/j.jmmm.2017.07.062.
[36] D.D. Dixit, A. Pattamatta, Natural convection heat transfer in a cavity filled with electrically conducting nano- particle suspension in the presence of magnetic field, *Phys. Fluids.* 31 (023302) (2019) 1–15. doi:10.1063/1.5080778.
[37] H.R. Ashorynejad, A. Shahriari, MHD natural convection of hybrid nanofluid in an open wavy cavity, *Results Phys.* 9 (2018) 440–455, https://doi.org/10.1016/j.rinp.2018.02.045.
[38] W.H. Leong, K.G.T. Hollands, A.P. Brunger, Experimental Nusselt numbers for a cubical-cavity benchmark problem in natural convection, *Int. J. Heat Mass Transf.* 42 (1998) 1979–1989, https://doi.org/10.1016/S0017-9310(98)00299-3.
[39] S.A. Adio, M. Mehrabi, M. Sharifpur, J.P. Meyer, Experimental investigation and model development for effective viscosity of MgO-ethylene glycol nanofluids by using dimensional analysis, FCM-ANFIS and GA-PNN techniques, *Int. Commun. Heat Mass Transf.* 72 (2016) 71–83, https://doi.org/10.1016/j.icheatmasstransfer.2016.01.005.
[40] M. Sharifpur, S.A. Adio, J.P. Meyer, Experimental investigation and model development for effective viscosity of Al2O3-glycerol nanofluids by using dimensional analysis and GMDH-NN methods, *Int. Commun. Heat Mass Transf.* 68 (2015) 208–219, https://doi.org/10.1016/j.icheatmasstransfer.2015.09.002.
[41] S.A. Adio, M. Sharifpur, J.P. Meyer, Investigation into effective viscosity, electrical conductivity, and pH of γ-Al2O3-glycerol nanofluids in Einstein concentration regime, *Heat Transf. Eng.* 36 (2015) 1241–1251, https://doi.org/10.1080/01457632.2015.994971.
[42] S.M. Mousavi, F. Esmaeilzadeh, X.P. Wang, Effects of temperature and particles volume concentration on the thermophysical properties and the rheological behavior of CuO/MgO/TiO2 aqueous ternary hybrid nanofluid Experimental investigation, *J. Therm. Anal. Calorim.* (2019), https://doi.org/10.1007/s10973-019-08006-0.
[43] S. Kannaiyan, C. Boobalan, A. Umasankaran, A. Ravirajan, S. Sathyan, T. Thomas, Comparison of experimental and calculated thermophysical properties of alumina/cupric oxide hybrid nanofluids, *J. Mol. Liq.* 244 (2017) 469–477, https://doi.org/10.1016/j.molliq.2017.09.035.
[44] M.S. Astanina, M. Kamel Riahi, E. Abu-Nada, M.A. Sheremet, Magnetohydrodynamic in partially heated square cavity with variable properties: discrepancy in experimental and theoretical conductivity correlations, *Int. J. Heat Mass Transf.* 116 (2018) 532–548, https://doi.org/10.1016/j.ijheatmasstransfer.2017.09.050.
[45] B. Berkovsky, V. Polevikov, Numerical study of problems on high-intensive free convection, in: *Proc. Int. Turbul. Buoyant Convect. Semin.*, 1977: pp. 443–455. http://www.elib.bsu.by/handle/123456789/10278.